Supporting Information For

Sc-HOPO: A Potential Construct for Use in Radioscandium Based Radiopharmaceuticals

Michael D Phipps[1,2,3,4a], Shelbie Cingoranelli[5a], N. V. S. Dinesh K. Bhupathiraju[3], Ali Younes[2], Minhua Cao[2], Vanessa A. Sanders[4], Michelle C. Neary[2], Matthew H. Daveny[2], Cathy S. Cutler[4], Gustavo E. Lopez[1,3], Shefali Saini[5], Candace C. Parker[5], Solana R. Fernandez[5], Jason S. Lewis[6], Suzanne E. Lapi[5], Lynn C. Francesconi[1,2], Melissa A. Deri[1,3*]

1. Ph.D. Program in Chemistry, The Graduate Center of the City University of New York, New York, NY 10016

2. Department of Chemistry, City University of New York Hunter College, 695 Park Avenue, New York, New York 10065

3. Department of Chemistry, Lehman College of the City University of New York, Bronx, NY 10468

4. Medical Isotope Research & Production Program, Collider-Accelerator Department, Brookhaven National Laboratory, Upton, NY, 11973, USA

5. Department of Radiology, University of Alabama at Birmingham, Birmingham, AL 35294

6. Program in Molecular Pharmacology and Chemistry, Memorial Sloan Kettering Cancer Center, New York, NY 10065

[*]Corresponding author: melissa.deri@lehman.cuny.edu

[a] = Michael D Phipps and Shelbie Cingoranelli contributed equally to this work.

Supporting Information Contents

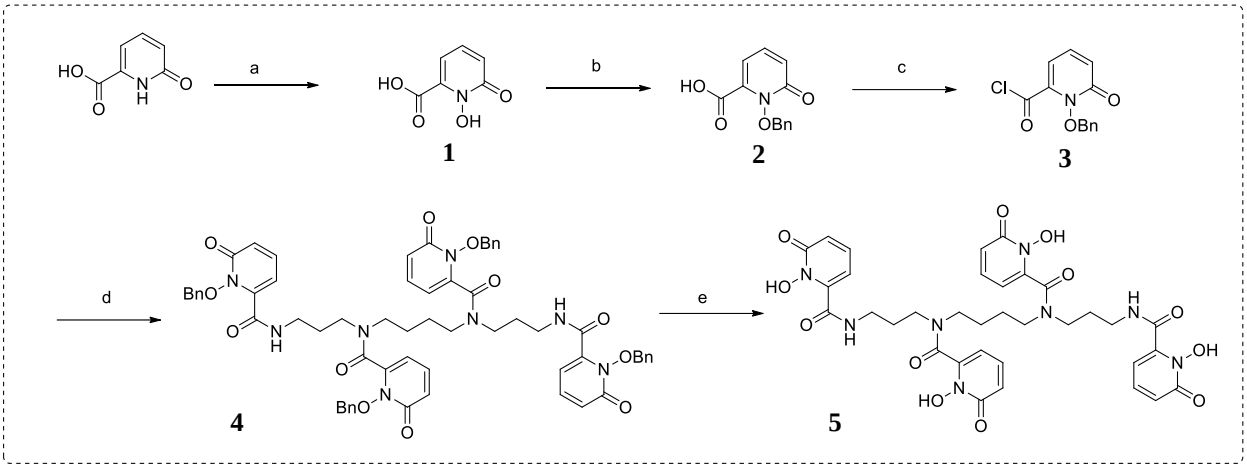

Scheme S1. Synthesis of 3,4,3-(LI-1,2-HOPO) (HOPO).

Reagents and conditions: a) Glacial acetic acid, trifluoroacetic acid, peracetic acid, 80°C, 1 day b) BnCl, K2CO3, MeOH, reflux at 60ºC for 16 h. c) $C_2O_2Cl_2$, DMF(cat), DCM, RT, 5 h d) Spermine, NEt_3, 1:1 toluene:DCM, 60 °C, 2 days e) BCl_3 in toulene, DCM, RT, 1day

HOPO Synthesis:

The synthesis of compound 5 or 3,4,3-Li(1,2-HOPO) was prepared based on the protocol described by Deri et al and Xu et al. with modification.^{1}H and ^{13}C NMR spectra were obtained using a Bruker Avance III 400MHz and Bruker Avance DRX 500MHz, Bruker Avance III 600 MHz; chemical shifts are expressed in ppm relative to $CDCl_3$ (7.26 ppm, ^{1}H; 77.0 ppm, ^{13}C), $(CD_3)_2CO$ (2.05 ppm, ^{1}H; 29.84 and 206.26 ppm, ^{13}C), CD_3OD (3.31 and 4.78 ppm, ^{1}H; 49.2 ppm, ^{13}C). Mass analyses were conducted at the CUNY Mass Spectrometry Facility at Hunter College on an Agilent iFunnel 6550 Q-ToF LC/MS System (for HRMS-ESI). The electrospray ionization was run in 95% methanol, with 0.1% formic acid. Reactions were monitored by TLC with Analtech Uniplate silica gel G/UV 254 precoated plates (0.2 mm). TLC plates were visualized by UV (254 nm), and by iodine vapour. Purification by Flash chromatography system from Biotag-Isolera™ was performed with Biotage ZIP Sphere 30-gram spherical silica 60 um. HPLC purification was performed with a Shimadzu GIST Shim Packed C18 Semi-preparative 10 x 250 mm column, and analysis was performed on a Kromasil Universal C18 4.6 x 250 mm column.

1-hydroxy-6-oxo-1,6-dihydropyridine-2-carboxylic acid (1). A stirring solution of 40 mL glacial acetic acid (42.30 g, 704.48 mmol, 9.8 eq) and 60 mL trifluoroacetic acid (88.52 g, 776.36 mmol, 10.8 eq) was prepared and added to a flask containing 10 g of 6-hydroxypicolinic acid (71.87 mmol, 1 eq). The mixture was stirred for around five minutes under nitrogen followed by the addition of 18.6 mL peracetic acid (21.01 g, 276.31 mmol, 1.23 eq). The peracetic acid was added in portions over 5 min. The mixture was stirred for one hour at room temperature and a cloudy solution was observed. The mixture was then placed under reflux at 80ºC for one day. In the process, the solution became clear and red, and a white precipitate was observed. The precipitate was collected by vacuum filtration, washed with cold methanol, and dried to yield

8.44 g (54.40 mmol, 76%); m.p. 176-177ºC; ^{1}H NMR (600 MHz, DMSO-d_6): δ = 6.64-6.98 (d, 2 H), 7.45-7.56 (s, 1 H), 10-12 (b, 2H). HRMS (H_2O): 156 (MH^+).

1-(benzyloxy)-6-oxo-1,6-dihydropyridine-2-carboxylic acid (2). 8.3 g of compound **1** (53.54 mmol, 1 eq.) and 14.79 g of anhydrous potassium carbonate (107.08 mmol, 2 eq.) was suspended in 150 mL dry methanol under nitrogen atmosphere. 6 mL benzyl chloride (9.12 g, 72.07 mmol, 1.2 eq) was added slowly, and the mixture was placed under reflux at 60ºC for 16 h. During this period, total dissolution of compound **1,** and a yellowish liquid that turned green, then brown over time was observed. The brownish liquid was filtered to separate potassium carbonate, and the liquid filtrate was evaporated to dryness. The brown residue was dissolved in water and acidified to pH = 2 employing 12 M HCl, and a white powder precipitated out of solution. The precipitate was isolated via vacuum filtration, washed with cold water and cold dichloromethane, and dried to yield 12.04 g (49.14 mmol, 92%); m.p. 176-177ºC; ^{1}H NMR (600 MHz, DMSO-d_6): δ = 5.29 (s, 2H), 6.56-6.57 (d, 1H), 6.73-6.75 (d, 1H), 7.41-7.52 (dd, 6H). HRMS (CH_3OH): 246 (MH+).

1-(benzyloxy)-6-oxo-1,6-dihydropyridine-2-carbonyl chloride (3). 6.048 g (24.69 mmol, 1 eq.) of compound **2** was suspended in 240 mL dry dichloromethane under nitrogen. The reaction mixture was placed under ice and 5.3 mL (7.83 g, 61.72 mmol, 2.5 eq.) oxalyl chloride was added dropwise, followed by 1 mL catalytic DMF extra dry. Fumes developed. The reaction mixture was left to stir at room temperature for 5 h, a period in which total dissolution of compound **2** was observed, and the solution became dark brown and clear. The reaction mixture was then evaporated to dryness and the green residue was used directly and immediately in the next reaction without further purification. HRMS (CH_3OH): 264 (MH+).

3,4,3-LI(1,2-HOPO)Bn (4). 0.135 g of spermine (0.667 mmol, 1 eq.) and 0.01 g (0.073 mmol, 0.10 eq.) of DMAP were suspended with 0.65 mL (0.473 g, 4.67 mmol, 7 eq.) trimethylamine over ice and stirred for 15 minutes. 50 mL of 1:1 dry toluene: dry dichloromethane was added and the solution was stirred for another 20 minutes until total solubility of spermine was observed. Compound 3, 0.87 g (33.366 mmol, 5 eq.), was dissolved in dry dichloromethane and 0.65 ml of trimethylamine. Then it was added dropwise to the spermine mixture over ice, and the reaction mixture was placed under reflux at 60ºC for 2 days. A color change was observed, from a tan color initially to a dark green after 16 hours. The final mixture was evaporated under reduced vacuum and was dissolved in DCM and washed twice with 10 % $NaHCO_3$. The organic phase was dried over anhydrous Na_2SO_4, filtered over cotton and evaporated under reduced vacuum. The crude compound was purified through flash column chromatography on a Biotage Isolera One system using 2-6% of methanol in dichloromethane eluent producing white crystalline foams compound **4**. Yield 60%, HRMS (CH_3OH): 1111.5 (MH+).

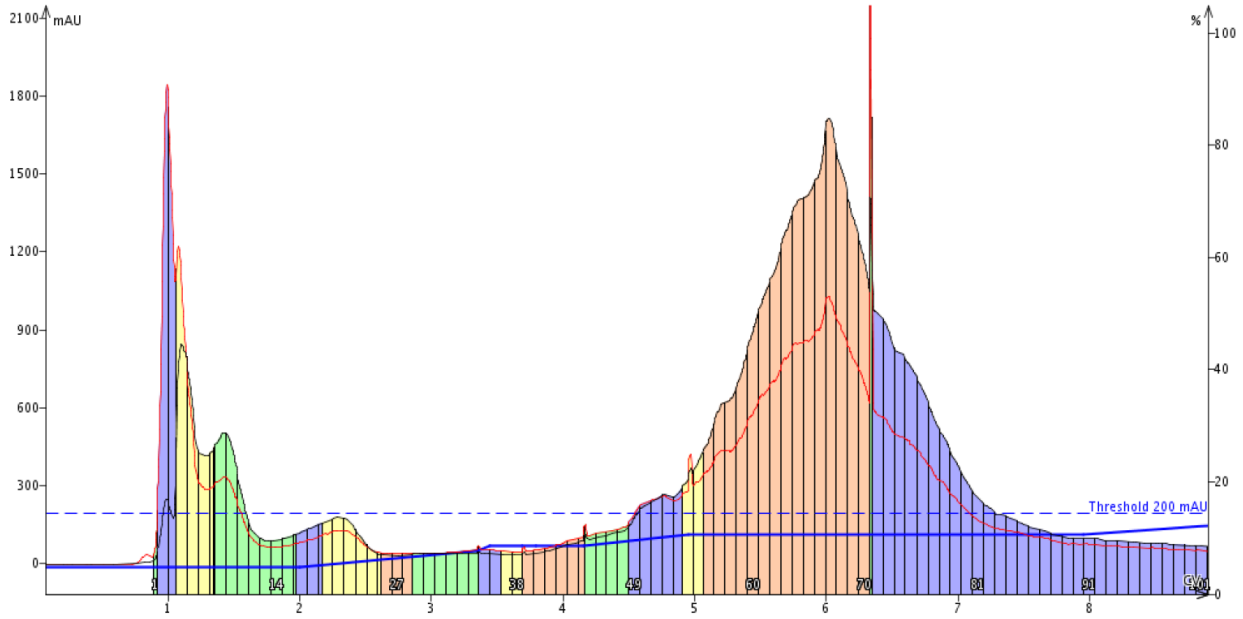

Figure S1: purification of compound 4 using an eluent of DCM: MeOH over a SNP-Silica gel column employing flash column chromatography.

3,4,3-LI(1,2-HOPO) (5). 0.065 g of compound **4** was dissolved in 70 mL dry dichloromethane and placed under ice. 1 mL BCl_3 in p-xylene was added to a vial containing 20 mL dry dichloromethane. The resulting solution was added to compound **4** slowly, in portions, over ice. The reaction was run at RT for 1 day, during which a light brown precipitate formed. The solid precipitate was filtered over vacuum (0.031 g crude weight) and purified over HPLC (10 × 250 mm Shimadzu Shim-packed GIST C18 column, H_2O/ACN + 0.1% TFA, 15-25% ACN over 20 min, 10 mL/min) OR (Waters Symmetry C18 Column, 100 Å, 5 µm, 4.6 mm × 100 mm, H_2O/ACN + 0.1% TFA, 5-35% ACN over 10 min, 10 mL/min) to yield compound **5.** HRMS (H_2O): 751 (MH+).

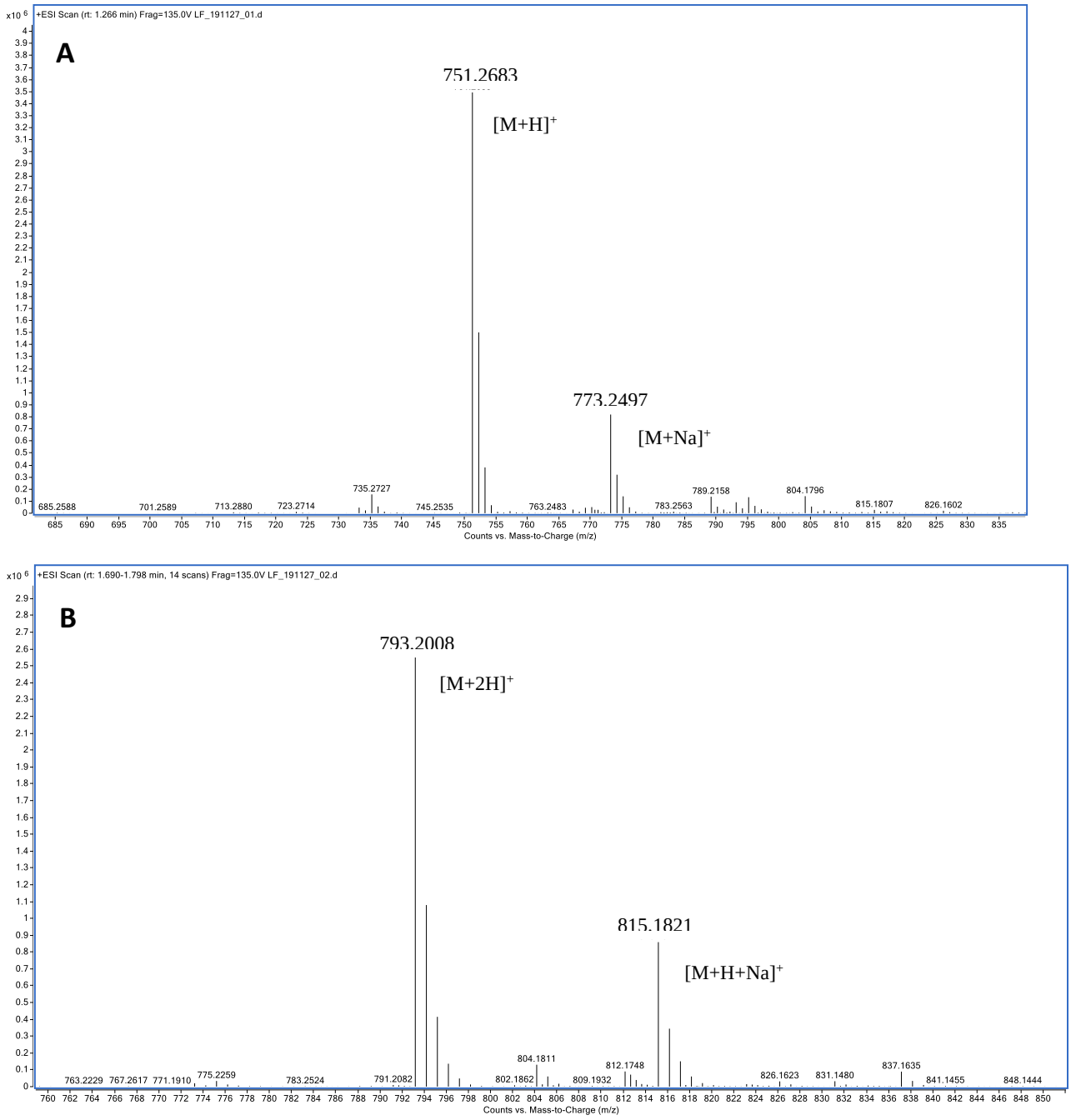

Figure S2. HRMS report for HOPO (**A**) and Sc-HOPO complex (**B**).

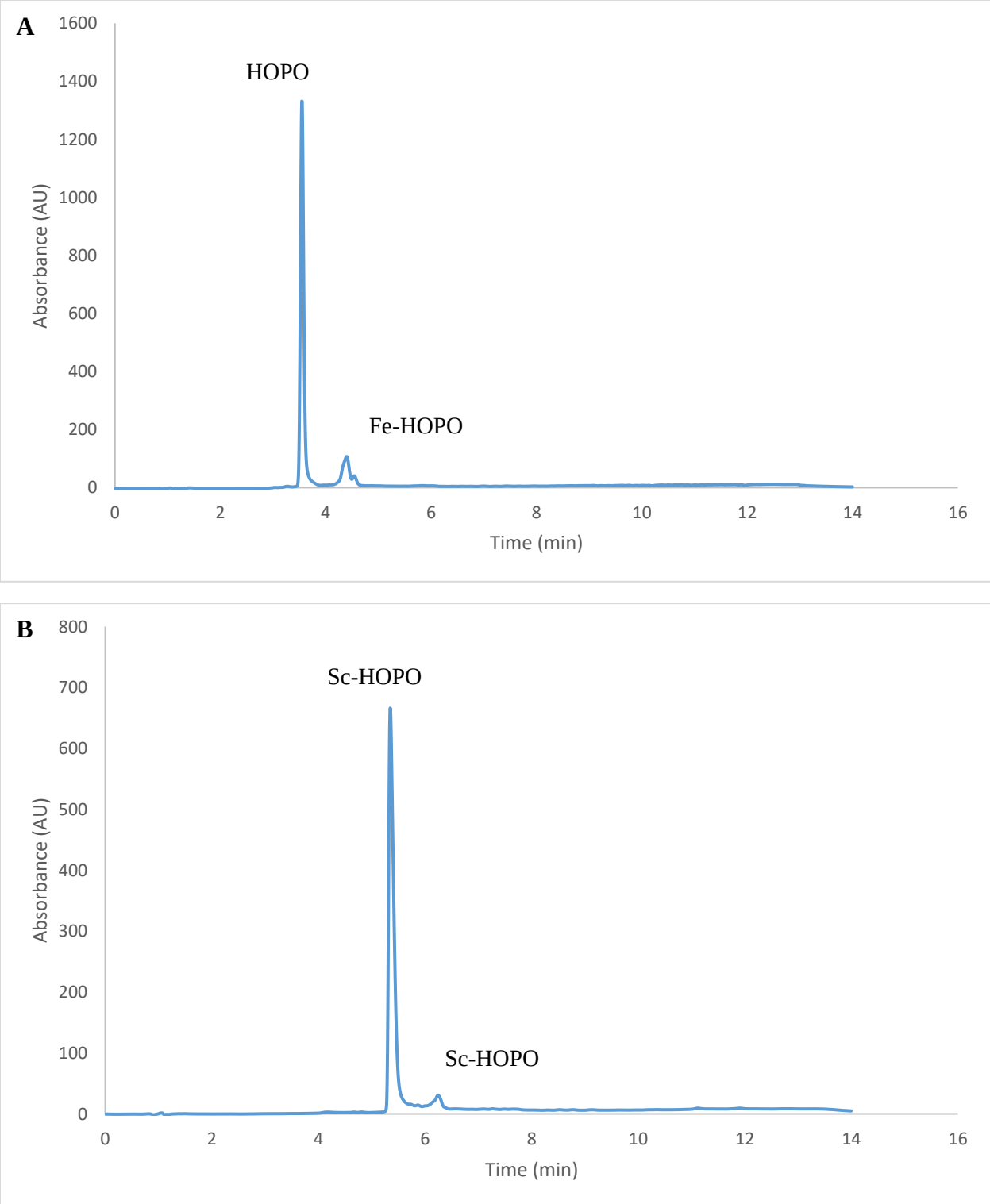

Figure S3. LC-MS chromatograms using UV detection at 254 nm for HOPO **(A)** and Sc-HOPO **(B)**

X-ray Structure Determination of Sc-HOPO. Colorless block crystals of $\{K(OH_2)_2[Sc(HOPO)]\}_2$ were grown by slow evaporation in a solution of K[Sc(HOPO)] in H_2O at pH 8. The solution was made basic using K_2CO_3. The addition of base was done to improve the solubility of the K[Sc(HOPO)]. X-ray diffraction data were collected on a Bruker X8 Kappa Apex II diffractometer using Mo Kα radiation. Crystal data, data collection and refinement parameters are summarized in Table S2. The structure was solved using a dual-space method and standard difference map techniques, and was refined by full-matrix least-squares procedures on F^2 with SHELXTL (Version 2018/3).[1,2] All hydrogen atoms bound to carbon were placed in calculated positions and refined with a riding model [U_{iso}(H) = 1.2–1.5U_{eq}(C)], while hydrogen atoms bound to nitrogen and oxygen were located on the difference map.

Additional strong peaks near the K atom and the water molecules bound to the K atom could be observed on the difference map; these were modeled as two-fold disorder of the $[K(OH_2)_2]^+$ moiety, with the occupancy of the two parts refining to 44% and 56%, respectively. Additional density was also observed in the difference map along the alkyl backbone of the ligand represented by C26-C29. This was likewise modeled as two-fold disorder, and the occupancies refined well to 25% and 75%, respectively.

One water molecule, represented by O61, H61A, and H61B, could be easily visualized in full on the difference map. This is likely due to the hydrogen bond O61-H61B···O32 anchoring it in place. There were additional electron density peaks in the empty space surrounding the primary molecule, but these did not refine well as oxygen atoms, and hydrogen atoms expected for water molecules could not be observed. Though the only solvent used during crystallization was water, models using methanol, ether, and DCM were also attempted in case adventitious molecules were introduced during the crystallization. However, these models also did not refine well. Therefore, all additional solvent molecules were treated as a diffuse contribution to the overall scattering without specific atom positions by SQUEEZE/PLATON.[3,4] Based on a volume of 1024 and an electron count of 382 between the two solvent voids, as well as the fact that water was the only solvent explicitly introduced during crystallization, the unit cell is estimated to contain anywhere from 24 to 38 additional disordered water molecules.

CCDC No. 2217080 contains the supplementary crystallographic data for this paper, with further details on the SQUEEZE/PLATON results and disorder refinement embedded into the .cif. These data can be obtained free of charge via http://www.ccdc.cam.ac.uk/conts/retrieving.html, or from the Cambridge Crystallographic Data Centre, 12 Union Road, Cambridge CB2 1EZ, UK; fax: (+44) 1223-336-033; or e-mail: deposit@ccdc.cam.ac.uk.

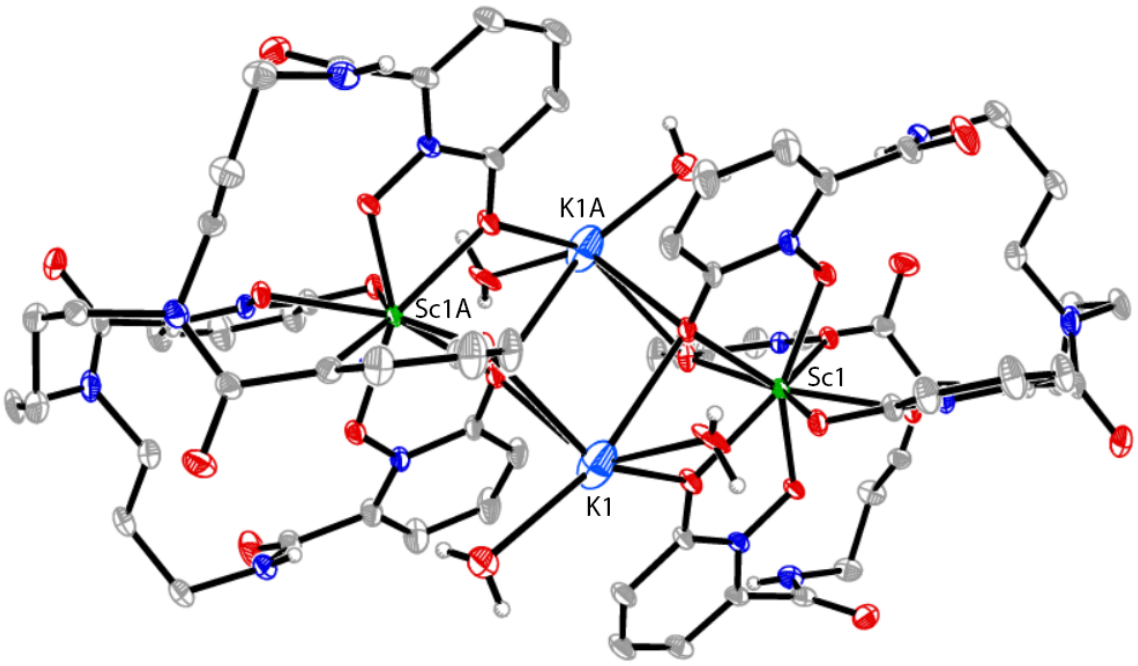

Figure S4. Molecular diagram of $\{K(OH_2)_2[Sc(HOPO)]\}_2$. Hydrogen atoms bound to carbon as well as disordered atoms are omitted for clarity. Atomic displacement parameters are displayed at the 30% probability level.

Table S1. Crystal, intensity collection, and refinement data.

	$\{K(OH_2)_2[Sc(HOPO)]\}_2 \cdot 2H_2O$
lattice	Monoclinic
formula	$C_{68}H_{80}K_2N_{16}O_{30}Sc_2$
formula weight	1769.60
space group	$P2_1/c$
a/Å	13.8985(8)
b/Å	12.6678(8)
c/Å	27.0216(15)
α/°	90
β/°	92.022(2)
γ/°	90
V/Å^3	4754.6(5)
Z	2
temperature (K)	130(2)
radiation (λ, Å)	0.71073
ρ (calcd.) g cm^{-3}	1.236
μ (Mo Kα), mm^{-1}	0.309
θ max, deg.	33.472
no. of data collected	176765
no. of data	18567
no. of parameters	627
R_1 [$I > 2\sigma(I)$]	0.0831
wR_2 [$I > 2\sigma(I)$]	0.2275
R_1 [all data]	0.1162
wR_2 [all data]	0.2673
GOF	1.062
R_{int}	0.0425

Table S2. Select bond lengths [Å] and angles [°] for $\{K(OH_2)_2[Sc(HOPO)]\}_2 \cdot 2H_2O$

K(1)-O(51)	2.397(15)
K(1)-O(41)	2.622(6)
K(1)-O(52)	2.631(13)
K(1)-O(31)#1	2.673(7)
K(1)-O(11)	2.958(7)
K(1)-O(11)#1	3.016(7)
K(1)-Sc(1)	4.196(6)
K(1)-Sc(1)#1	4.200(6)
K(1)-K(1)#1	4.927(14)
O(51)-H(51A)	0.840(2)
O(51)-H(51B)	0.840(2)
O(52)-H(52A)	0.840(2)
O(52)-H(52B)	0.840(2)
Sc(1)-O(42)	2.1790(17)
Sc(1)-O(12)	2.1935(17)
Sc(1)-O(31)	2.1953(19)
Sc(1)-O(21)	2.211(2)
Sc(1)-O(41)	2.2373(17)
Sc(1)-O(32)	2.2385(17)
Sc(1)-O(22)	2.2529(17)
Sc(1)-O(11)	2.2658(17)
N(12)-H(12)	0.91(4)
N(42)-H(42)	0.77(4)
O(51)-K(1)-O(41)	94.6(3)
O(51)-K(1)-O(52)	108.7(4)
O(41)-K(1)-O(52)	134.4(4)
O(51)-K(1)-O(31)#1	101.9(4)
O(41)-K(1)-O(31)#1	133.4(3)
O(52)-K(1)-O(31)#1	80.2(3)
O(51)-K(1)-O(11)	76.3(3)
O(41)-K(1)-O(11)	56.41(13)
O(52)-K(1)-O(11)	165.7(4)

O(31)#1-K(1)-O(11)	85.7(2)
O(51)-K(1)-O(11)#1	139.7(4)
O(41)-K(1)-O(11)#1	82.75(17)
O(52)-K(1)-O(11)#1	101.1(3)
O(31)#1-K(1)-O(11)#1	56.79(14)
O(11)-K(1)-O(11)#1	68.88(15)
O(51)-K(1)-Sc(1)	77.1(3)
O(41)-K(1)-Sc(1)	27.74(9)
O(52)-K(1)-Sc(1)	161.6(4)
O(31)#1-K(1)-Sc(1)	116.3(2)
O(11)-K(1)-Sc(1)	31.25(6)
O(11)#1-K(1)-Sc(1)	83.15(13)
O(51)-K(1)-Sc(1)#1	127.1(4)
O(41)-K(1)-Sc(1)#1	113.82(19)
O(52)-K(1)-Sc(1)#1	82.7(3)
O(31)#1-K(1)-Sc(1)#1	27.22(8)
O(11)-K(1)-Sc(1)#1	83.74(16)
O(11)#1-K(1)-Sc(1)#1	31.50(7)
Sc(1)-K(1)-Sc(1)#1	108.13(15)
O(51)-K(1)-K(1)#1	108.9(4)
O(41)-K(1)-K(1)#1	65.83(15)
O(52)-K(1)-K(1)#1	134.4(4)
O(31)#1-K(1)-K(1)#1	67.63(18)
O(11)-K(1)-K(1)#1	34.82(10)
O(11)#1-K(1)-K(1)#1	34.06(9)
Sc(1)-K(1)-K(1)#1	54.11(11)
Sc(1)#1-K(1)-K(1)#1	54.03(12)
O(42)-Sc(1)-O(12)	149.84(6)
O(42)-Sc(1)-O(31)	84.99(7)
O(12)-Sc(1)-O(31)	104.04(8)
O(42)-Sc(1)-O(21)	109.10(7)
O(12)-Sc(1)-O(21)	78.95(7)
O(31)-Sc(1)-O(21)	147.03(7)
O(42)-Sc(1)-O(41)	70.50(6)
O(12)-Sc(1)-O(41)	139.00(7)
O(31)-Sc(1)-O(41)	79.64(7)

O(21)-Sc(1)-O(41)	77.59(7)
O(42)-Sc(1)-O(32)	77.52(6)
O(12)-Sc(1)-O(32)	78.56(7)
O(31)-Sc(1)-O(32)	70.63(6)
O(21)-Sc(1)-O(32)	140.41(6)
O(41)-Sc(1)-O(32)	137.77(7)
O(42)-Sc(1)-O(22)	78.19(6)
O(12)-Sc(1)-O(22)	77.76(7)
O(31)-Sc(1)-O(22)	143.33(7)
O(21)-Sc(1)-O(22)	69.63(6)
O(41)-Sc(1)-O(22)	123.30(7)
O(32)-Sc(1)-O(22)	74.00(6)
O(42)-Sc(1)-O(11)	140.24(6)
O(12)-Sc(1)-O(11)	69.57(6)
O(31)-Sc(1)-O(11)	75.18(7)
O(21)-Sc(1)-O(11)	75.35(7)
O(41)-Sc(1)-O(11)	72.22(6)
O(32)-Sc(1)-O(11)	125.05(7)
O(22)-Sc(1)-O(11)	135.74(6)
O(42)-Sc(1)-K(1A)#1	118.38(5)
O(12)-Sc(1)-K(1A)#1	81.87(5)
O(31)-Sc(1)-K(1A)#1	37.65(6)
O(21)-Sc(1)-K(1A)#1	113.19(6)
O(41)-Sc(1)-K(1A)#1	77.19(6)
O(32)-Sc(1)-K(1A)#1	95.30(6)
O(22)-Sc(1)-K(1A)#1	158.48(5)
O(11)-Sc(1)-K(1A)#1	38.11(6)
O(42)-Sc(1)-K(1A)	106.47(5)
O(12)-Sc(1)-K(1A)	103.48(5)
O(31)-Sc(1)-K(1A)	79.43(6)
O(21)-Sc(1)-K(1A)	68.12(6)
O(41)-Sc(1)-K(1A)	36.13(5)
O(32)-Sc(1)-K(1A)	149.43(6)
O(22)-Sc(1)-K(1A)	136.53(6)
O(11)-Sc(1)-K(1A)	36.70(5)
K(1A)#1-Sc(1)-K(1A)	55.61(7)

O(42)-Sc(1)-K(1)	103.23(12)
O(12)-Sc(1)-K(1)	105.94(12)
O(31)-Sc(1)-K(1)	86.80(10)
O(21)-Sc(1)-K(1)	61.35(10)
O(41)-Sc(1)-K(1)	33.07(12)
O(32)-Sc(1)-K(1)	157.34(10)
O(22)-Sc(1)-K(1)	128.58(10)
O(11)-Sc(1)-K(1)	42.63(12)
O(42)-Sc(1)-K(1)#1	117.64(12)
O(12)-Sc(1)-K(1)#1	79.24(13)
O(31)-Sc(1)-K(1)#1	33.85(11)
O(21)-Sc(1)-K(1)#1	119.40(9)
O(41)-Sc(1)-K(1)#1	83.67(12)
O(32)-Sc(1)-K(1)#1	87.58(9)
O(22)-Sc(1)-K(1)#1	152.91(12)
O(11)-Sc(1)-K(1)#1	44.06(9)
K(1)-Sc(1)-K(1)#1	71.87(15)

Symmetry transformations used to generate equivalent atoms:

#1 -x+1,-y+1,-z+1

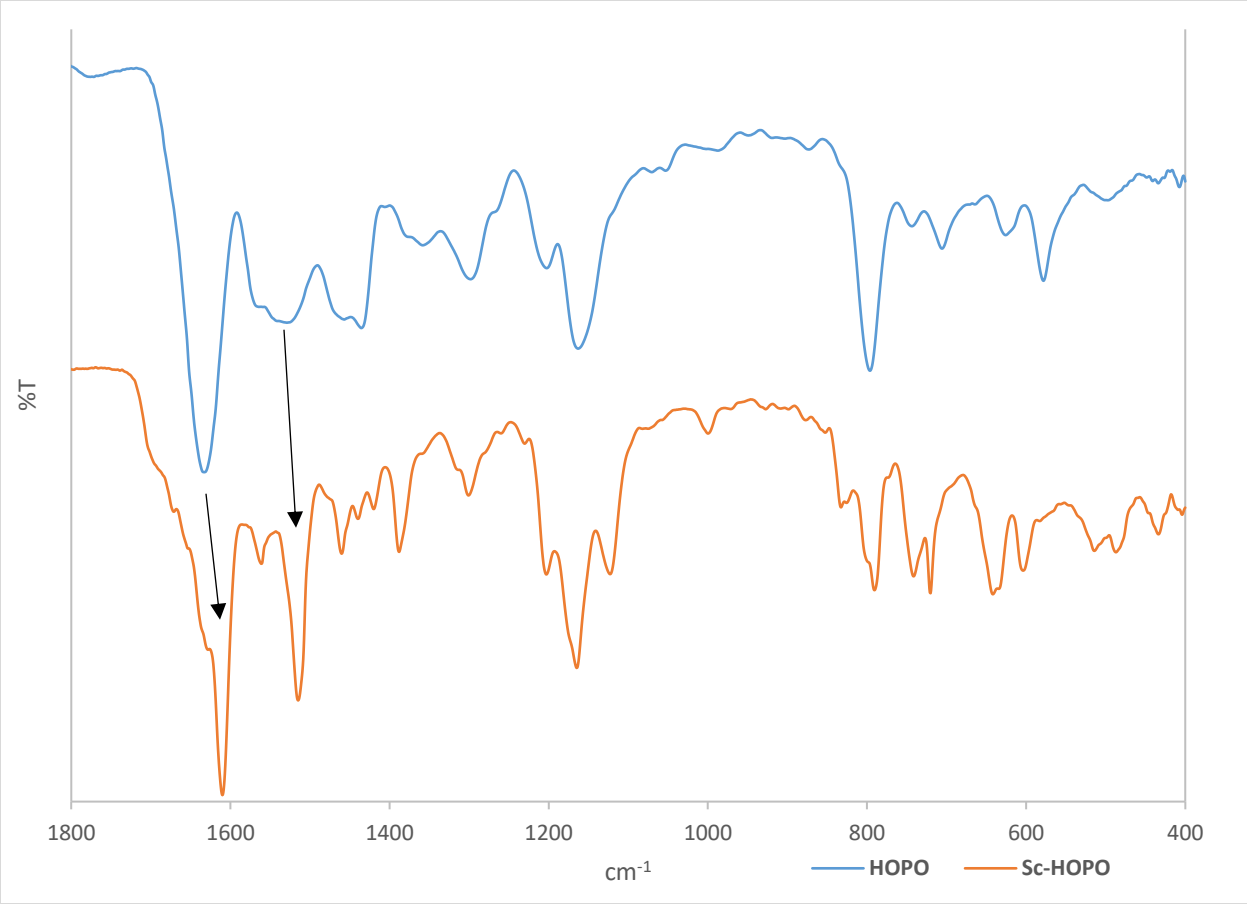

Figure S5. FT-IR spectra of HOPO (top, blue) and Sc-HOPO (bottom, orange). Solid powder samples of each molecule were pressed under a mechanical arm and scanned via attenuated total reflectance (ATR). Two points identified in the figure are characteristic of HOPO bound to a metal center with corresponding changes in the spectrum (1633 to 1610, 1529 to 1515 cm^{-1}). These shifts are characteristic of hydroxypyridinonate binding to a metal.

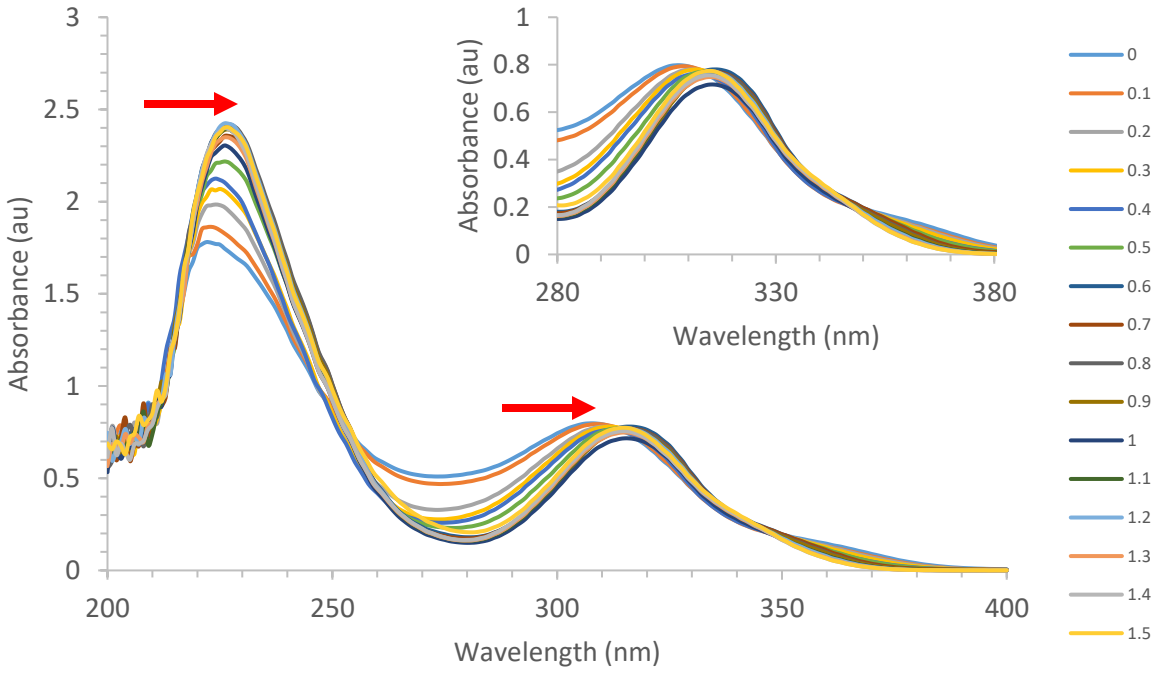

Figure S6. Overlayed UV-Vis spectra of HOPO and Sc-HOPO with increasing equivalents of Sc^{3+}. The red arrows indicate the change in peak position as Sc^{3+} equivalents are added. Because of the fast reaction kinetics, there was only a short delay in between titrations and the collection of UV-vis data.

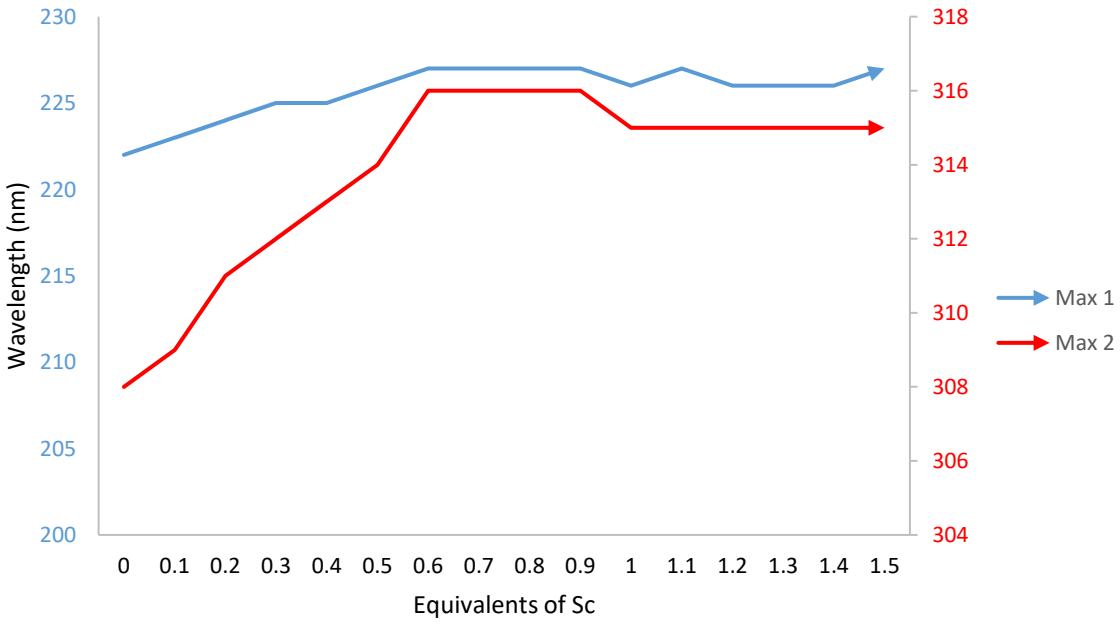

Figure S7. UV-Vis absorbance maxima vs. equivalents of Sc^{3+}. Max 1 is the peak of the highest intensity. Max 2 is the second highest intensity peak. The x-axis refers to the ratio of Sc-HOPO in a reaction.

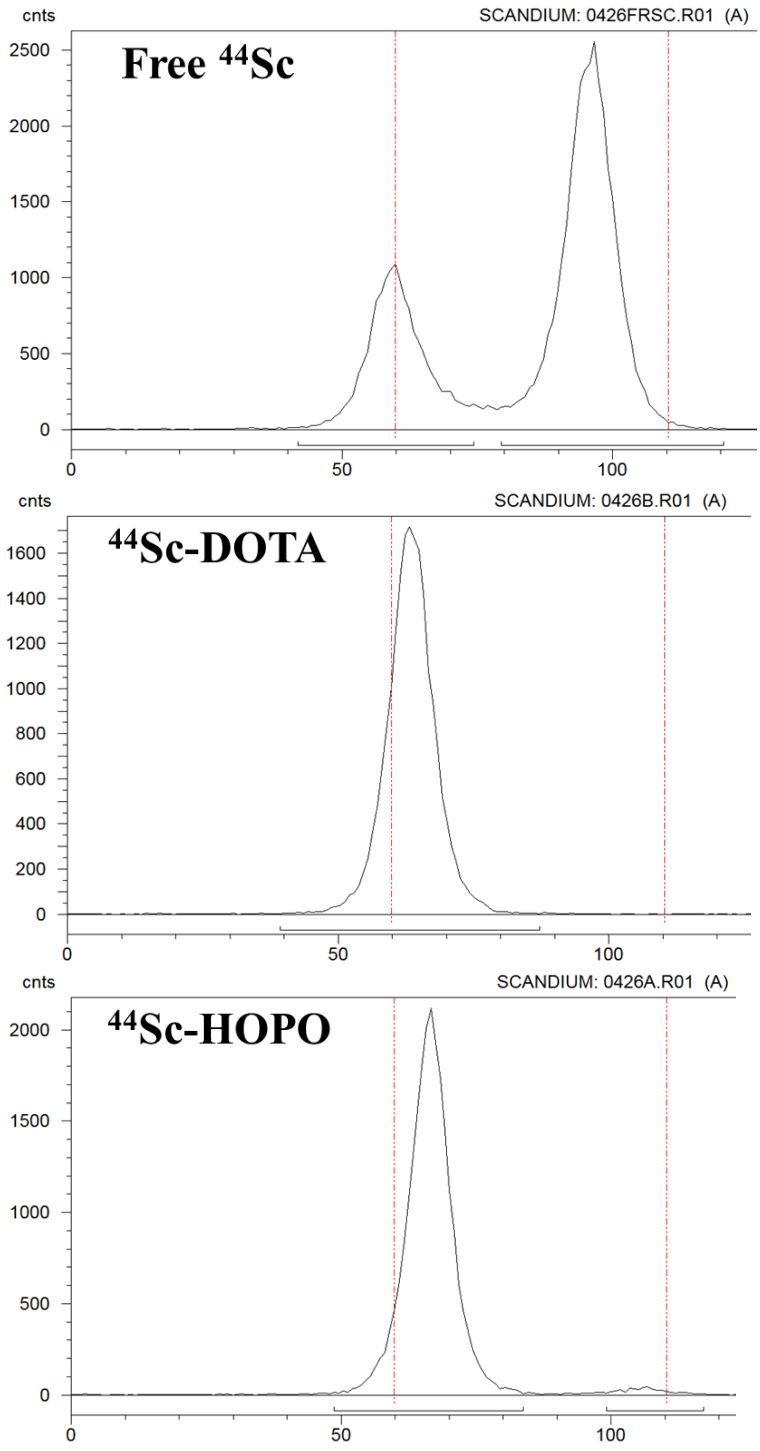

Figure S8. ITLC profiles of free ^{44}Sc, ^{44}Sc-DOTA, and ^{44}Sc-HOPO radiolabeling solutions. ITLC were run in 50 mM EDTA at pH 5 on plastic backed silica gel plates.

Table S3: [^{47}Sc]-HOPO Biodistribution results (n=4)								
Tissue	**10 minute (%ID/g)**		**1 hour (%ID/g)**		**4 hour (%ID/g)**		**24 hour (%ID/g)**	
	Average	**St.D**	**Average**	**St.D**	**Average**	**St.D**	**Average**	**St.D**
Blood	**2.14**	**3.91**	**0.09**	**0.05**	**0.06**	**0.02**	**0.05**	**0.01**
Heart	**0.33**	**0.34**	**0.08**	**0.03**	**0.04**	**0.02**	**0.07**	**0.07**
Lungs	**3.39**	**1.07**	**2.65**	**1.83**	**3.67**	**1.58**	**0.85**	**0.79**
Pancreas	**0.34**	**0.22**	**0.06**	**0.04**	**0.03**	**0.01**	**0.04**	**0.02**
Spleen	**0.92**	**0.61**	**0.32**	**0.14**	**0.94**	**0.72**	**0.98**	**1.03**
Stomach	**2.55**	**1.98**	**1.06**	**1.96**	**0.03**	**0.03**	**0.06**	**0.04**
Liver	**4.03**	**1.98**	**1.12**	**1.368**	**0.76**	**0.11**	**0.47**	**0.19**
Kidney	**1.51**	**0.71**	**1.22**	**0.41**	**0.67**	**0.11**	**0.31**	**0.16**
S. intestines	**25.77**	**3.26**	**10.44**	**4.87**	**0.07**	**0.01**	**0.03**	**0.02**
L. Intestines	**0.21**	**0.19**	**53.11**	**30.22**	**18.89**	**2.55**	**0.31**	**0.36**
Fat	**1.25**	**0.84**	**0.29**	**0.32**	**0.03**	**0.02**	**0.02**	**0.02**
Skin	**0.71**	**0.41**	**0.19**	**0.31**	**0.02**	**0.02**	**0.02**	**0.01**
Muscle	**0.58**	**0.52**	**0.55**	**0.86**	**0.07**	**0.05**	**0.11**	**0.13**
Femur	**0.22**	**0.13**	**0.18**	**0.11**	**0.15**	**0.07**	**0.18**	**0.11**
Brain	**0.09**	**0.10**	**0.02**	**0.01**	**0.01**	**0.01**	**0.01**	**0.01**
Tail	**0.61**	**0.22**	**0.64**	**0.74**	**0.03**	**0.06**	**0.01**	**0.01**

Table S4: [^{43}Sc]-HOPO Biodistribution results at 90 minutes (n=4) (%ID/g)		
Tissue	**Average**	**St.D**
Blood	**0.27**	**0.01**
Heart	**0.18**	**0.03**
Lungs	**0.81**	**0.28**
Pancreas	**0.36**	**0.49**
Spleen	**1.73**	**1.32**
Stomach	**0.27**	**0.27**
Liver	**5.81**	**4.82**
Kidney	**0.88**	**0.13**
S. intestines	**43.70**	**19.11**
L. Intestines	**36.51**	**2.37**
Fat	**0.69**	**0.59**
Skin	**0.41**	**0.47**
Muscle	**0.11**	**0.05**
Femur	**0.69**	**0.35**
Brain	**0.06**	**0.02**
Tail	**0.09**	**0.01**

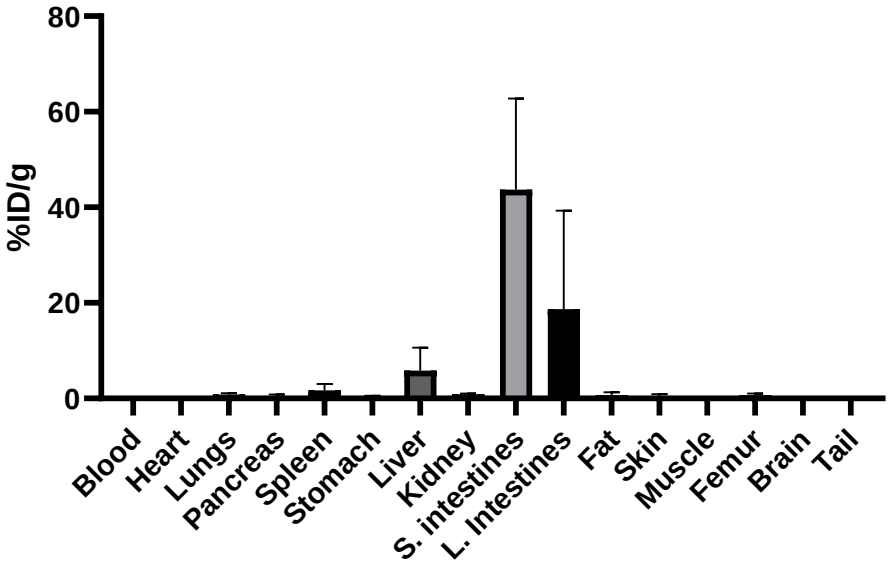

Figure S9. Biodistribution of 100 μCi injections of [^{43}Sc]Sc-HOPO in female Balb/c mice after a 90-minute dynamic imaging.

Table S5: [^{47}Sc]$ScCl_3$ biodistribution at 1 hour (n=4) (%ID/g)		
Tissue	**Average**	**St.D**
Blood	**4.75**	**0.76**
Heart	**12.50**	**3.02**
Lungs	**13.01**	**1.91**
Pancreas	**4.03**	**1.65**
Spleen	**17.13**	**2.51**
Stomach	**1.83**	**0.65**
Liver	**10.87**	**0.94**
Kidney	**12.63**	**1.33**
S. intestines	**4.45**	**0.22**
L. Intestines	**2.48**	**0.68**
Fat	**9.95**	**0.45**
Skin	**1.68**	**0.18**
Muscle	**8.69**	**0.43**
Femur	**10.52**	**1.85**
Brain	**1.14**	**0.41**
Tail	**1.81**	**0.53**

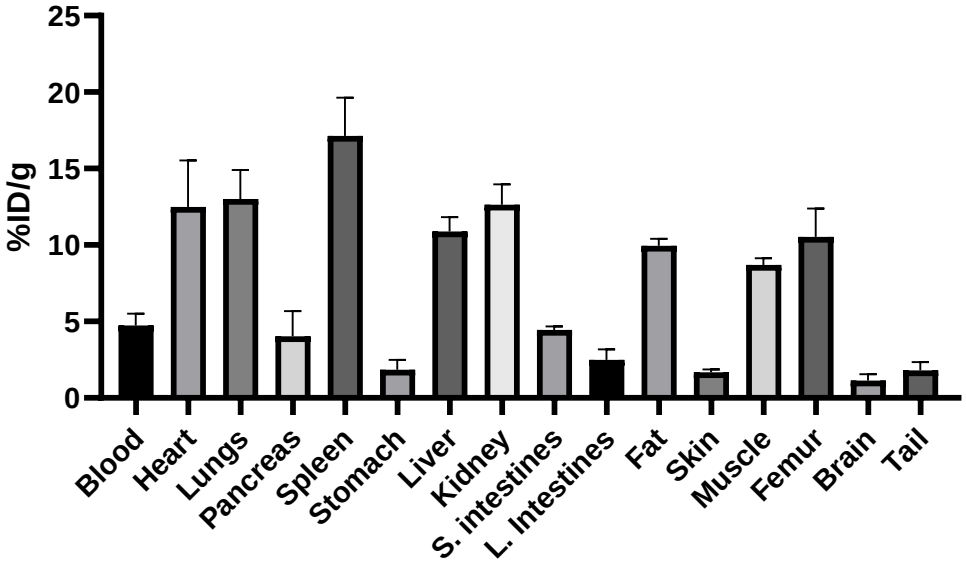

Figure S10. Biodistribution of 10 μCi injections of [^{47}Sc]$ScCl_3$ in female Balb/c mice at 1 hour post injections.

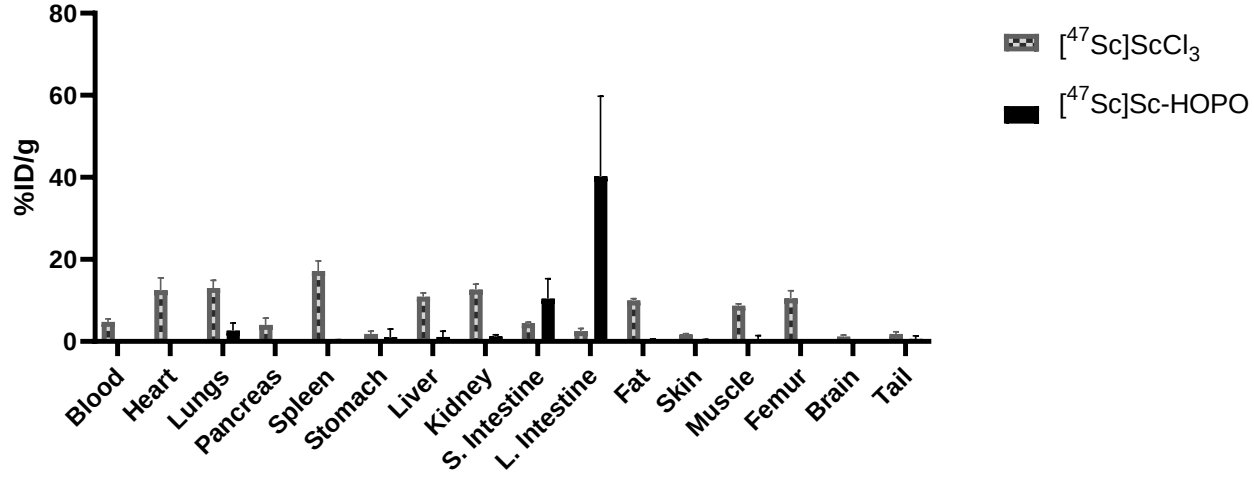

Figure S11. Biodistribution of 10 μCi injections of [^{47}Sc]$ScCl_3$ and [^{47}Sc]Sc-HOPO in female Balb/c mice at 1 hour post injections.

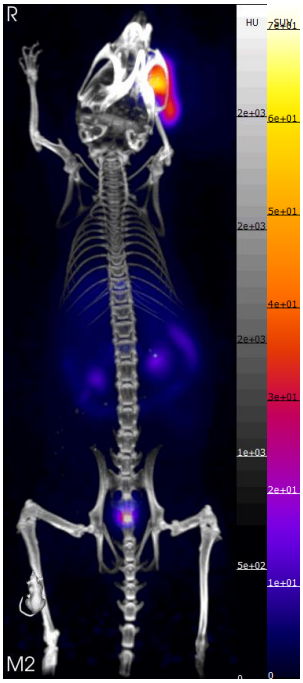

Figure S12: PET/CT maximum intensity projection movie of a Balb/c mouse for a 90-minute dynamic scan immediately after injection of approximately 100 μCi of [^{43}Sc]-HOPO. Movie file has been uploaded as a Web Enhanced Object.

References

1. Sheldrick, G. M. SHELXTL, An Integrated System for Solving, Refining, and Displaying Crystal Structures from Diffraction Data; University of Göttingen, Göttingen, Federal Republic of Germany, 1981.

2. Sheldrick, G. M. Acta Cryst. 2015, A71, 3-8.

3. A.L.Spek (2005) PLATON, A Multipurpose Crystallographic Tool, Utrecht University, Utrecht, The Netherlands.

4. A.L.Spek, J. Appl. Cryst. 2003, 36, 7-13.